Langevin simulations of quantum systems

R. Badii,* T. Schneider, and M. P. Soerensen
IBM Zurich Research Laboratory, 8803 Rüschlikon, Switzerland
(Received 4 November 1985; revised manuscript received 2 June 1986)

We explore the potential of the Langevin simulation of quantum systems. A generalized quantum sine-Gordon chain, a generalized Toda chain, and impenetrable bosons on a ring are treated specifically to estimate low-lying excitation energies from the long-time behavior of the Langevin process. In the sine-Gordon case, we investigated the dependence of the bound-state frequency on the coupling constant, while in the Toda chain the phonon dispersion curves are obtained for different coupling constants. Finally, for impenetrable bosons the estimated dynamic form factor for density fluctuations is compared with exact results.

I. INTRODUCTION AND FORMALISM

In this work, we present Langevin simulation results for quantum systems. Specifically, we consider a generalized sine-Gordon chain, a generalized Toda chain, and free impenetrable bosons on a ring. The link between a system evolving according to the Langevin equation and a quantum problem is established via the Fokker-Planck equation which can be reduced to an imaginary Schrödinger equation by appropriately choosing the variance of the random force in the Langevin equation.[1–5] As a result, a system evolving according to the Langevin equation and specified by its potential energy W is related to a quantum model with potential energy V, where $V(W)$, as well as the ground-state wave function with zero energy, are known. Consequently, ground-state properties and the energy spectrum of the quantum system can be investigated by simulating correlation functions in the stationary Langevin process.[2,3] This route is adopted by considering a sine-Gordon and Toda chain with potential energy W and evolving according to the Langevin equations. Conversely, for a given quantum problem with potential energy V, the drift force resulting from the potential W must be obtained from an independent solution of the Schrödinger equation for the ground state.[2,4–6] The ground-state energy and the wave function allow the construction of associated Langevin equations, again providing estimates for the ground-state properties and the energy spectrum. This route will be illustrated for impenetrable bosons on a ring, where the ground-state wave function is known.[7]

Other interesting aspects of this relationship between Langevin dynamics and an associated quantum system are:

(i) The critical dynamics of a d-dimensional time-dependent Ginzburg-Landau model can be mapped onto the static critical properties of an associated quantum model and its $(d+1)$-dimensional static and classical counterpart.[4,5]

(ii) Critical dynamics can be obtained from statics. Accordingly, the dynamic scaling hypothesis is traced back to static anisotropic scaling.[8,9]

(iii) Construction of quantum models with soluble ground-state properties.[10]

The paper is organized as follows. Next, we sketch the formalism to unravel the relationship between the model evolving according to the Langevin equations and the associated quantum system and vice versa. In Sec. II, we introduce the model system and derive some ground-state properties. The numerical results of the Langevin simulation are discussed in Sec. III. For a sketch of the numerical technique, we refer to the Appendix.

To sketch the formalism, we consider a one-dimensional N-particle system. The time evolution is assumed to be given by the Langevin equations

$$\dot{x}_l=\frac{dx_l}{dt}=-\frac{\partial W}{\partial x_l}+\eta_l(t),\quad l=1,\ldots,N \tag{1}$$

with the drift forces $F_l=-\partial W/\partial x_l$ and the random forces η_l, with correlations

$$\langle\eta_l(t)\rangle=0,\quad \langle\eta_l(t)\eta_{l'}(t')\rangle=\sigma\delta_{ll'}\delta(t-t')\ . \tag{2}$$

The associated Fokker-Planck equation for the probability density $P(x_1,\ldots,x_N;t)$,

$$\frac{\partial P}{\partial t}=\sum_l\frac{\partial}{\partial x_l}\left[\frac{\partial W}{\partial x_l}P\right]+\frac{\sigma}{2}\sum_l\frac{\partial^2 P}{\partial x_l^2}\ , \tag{3}$$

in the stationary equilibrium state admits the solution

$$P_{\rm eq}\sim\exp\left[-\frac{2W}{\sigma}\right]\ . \tag{4}$$

Invoking the transformation

$$P(x_1,\ldots,x_N;t)=P_{\rm eq}^{1/2}\psi(x_1,\ldots,x_N;t)\ , \tag{5}$$

it reduces to the imaginary-time Schrödinger equation

$$-\frac{\partial\psi}{\partial t}=\mathscr{H}\psi\ , \tag{6}$$

with Hamiltonian

$$\mathscr{H}=-\frac{\sigma}{2}\sum_l\frac{\partial^2}{\partial x_l^2}+V\ . \tag{7}$$

The potentials W [Eq. (1)] and V are related by the Riccati-type equation:

$$V=\frac{1}{2\sigma}\sum_l\left[\frac{\partial W}{\partial x_l}\right]^2-\tfrac{1}{2}\sum_l\frac{\partial^2 W}{\partial x_l^2}\ . \tag{8}$$

The associated eigenvalue problem

$$\mathscr{H}\varphi_n=\lambda_n\varphi_n \tag{9}$$

yields a non-negative energy spectrum, with the ground state

$$\lambda_0=0,\quad \varphi_0\sim P_{\rm eq}^{1/2}=\exp\left[-\frac{W}{\sigma}\right]. \tag{10}$$

This set of equations forms the framework for the correspondence between the Langevin process and a quantum problem. In fact, considering the Schrödinger equation

$$i\frac{\partial\psi}{\partial t}=\frac{1}{\hbar}\mathscr{H}\psi,\quad \mathscr{H}=-\frac{\hbar^2}{2m}\sum_l\frac{\partial^2}{\partial x_l^2}+\tilde{V}(x_1,\ldots,x_N) \tag{11}$$

and setting

$$\psi\sim\varphi_n e^{-\lambda_n t}, \tag{12}$$

we obtain an eigenvalue problem identical to the corresponding Fokker-Planck expressions (7) and (9), provided

$$t\to -it,\quad \frac{\hbar}{m}=\sigma,\quad \frac{1}{\hbar}\tilde{V}=V\ . \tag{13}$$

The general solution of the Fokker-Planck equation (3) can then be expressed as

$$P(x,t)=\varphi_0^2+\varphi_0\sum_{n=1}^{\infty}C_n\varphi_n e^{-\lambda_n t}\ . \tag{14}$$

To simplify the notation, we consider here one particle only. Because the λ_n are real and non-negative, it follows that

$$\lim_{t\to\infty}P(x,t)=\varphi_0^2=P_{\rm eq}\sim\exp\left[-\frac{2W}{\sigma}\right]. \tag{15}$$

By invoking the initial condition

$$P(x,0)=\delta(x-x') \tag{16}$$

and denoting the solution of the Fokker-Planck equation (3) as $P(x,t,\mid x')$, we obtain

$$P(x,t\mid x')=\varphi_0(x)\sum_{n=0}^{\infty}\frac{\varphi_n(x')}{\varphi_0(x')}\varphi_n(x)e^{-\lambda_n t}, \tag{17}$$

reducing for $t=0$ to Eq. (16). Assuming then stationarity of the Langevin process

$$\langle x(t+\tau)x(\tau)\rangle=\langle x(t)x(0)\rangle\ , \tag{18}$$

two time correlation functions can be expressed as

$$\begin{aligned}\langle x(t)x(0)\rangle&=\int dx\int dx'\,xx'P_{\rm eq}(x')P(x,t\mid x')\\&=\sum_{n=0}^{\infty}\mid\langle 0\mid x\mid n\rangle\mid^2 e^{-\lambda_n t}\end{aligned} \tag{19}$$

reducing to

$$\begin{aligned}\langle x(0)x(0)\rangle&=\sum_{n=0}^{\infty}\mid\langle 0\mid x\mid n\rangle\mid^2\\&=\langle 0\mid x^2\mid 0\rangle=\int\varphi_0^2x^2dx\ ,\\\lim_{t\to\infty}\langle x(t)x(0)\rangle&=\mid\langle 0\mid x\mid 0\rangle\mid^2=\left[\int\varphi_0^2 x dx\right]^2,\end{aligned} \tag{20}$$

where $\langle\ \rangle$ denotes an average over the Gaussian-noise ensemble. The convergence criterium (15) ensures that the ensemble is ergodic in the sense that time and ensemble averages are identical,

$$\begin{aligned}\langle x(t)x(0)\rangle&=\lim_{t_n-t_m\to\infty}\frac{1}{t_n-t-t_m}\int_{t_m}^{t_n-t}x(t')x(t'+t)dt'\\&=\sum_n\mid\langle 0\mid x\mid n\rangle\mid^2 e^{-\lambda_n t},\end{aligned} \tag{21}$$

and

$$\langle x^2\rangle=\lim_{t_n-t_m\to\infty}\frac{1}{t_n-t_m}\int_{t_m}^{t_n}x^2(t')dt'\ . \tag{22}$$

The long-time behavior of the Langevin process then provides estimates for the lowest eigenvalue λ_{nL} with $\langle 0\mid x^P\mid nL\rangle\neq 0$ from

$$\langle x^P(t)x^P(0)\rangle\to\langle 0\mid x^P\mid nL\rangle e^{-\lambda_{nL}t}\ \text{ as } t\to\infty\ . \tag{23}$$

Up to now, we have outlined the relationship between model W, defined by the Langevin equation (1) and the associated quantum system [Eq. (7)]. To construct the Langevin equation for a given quantum system, we can still use Eq. (15), giving the classical potential W in terms of a given quantum ground state. Clearly, the ground-state energy of a given quantum problem will not vanish in general. This is easily seen by substituting Eq. (15) into Eq. (6) yielding the modified Riccati-type equation

$$V(x)-\lambda_0=\frac{1}{2\sigma}\left[\frac{\partial W}{\partial x}\right]^2-\frac{1}{2}\frac{\partial^2 W}{\partial x^2}\ . \tag{24}$$

Thus, for a given quantum system, the drift force in the associated Langevin equation is obtained from

$$\frac{\partial W}{\partial x}=-\sigma\frac{\partial\ln\varphi_0}{\partial x}\ , \tag{25}$$

but the eigenvalues λ_n in Eq. (21) must be replaced by $\lambda_n\to\lambda_n-\lambda_0$.

For the purpose of numerical simulations, the outlined relationship between the Langevin equation and the associated quantum problem can be used in two ways: (i) the potential V entering the quantum problem is constructed from a given W by means of the Riccati equation (8); (ii) for a given quantum problem, the potential W entering the Langevin equation must be obtained from an independent method providing the ground-state wave function and energy [Eq. (25)]. The long-time behavior of the Langevin process then provides information on the ground-state properties and eigenvalue spectrum of the quantum problem.

II. MODEL SYSTEMS AND GROUND-STATE PROPERTIES

Before turning to the specific models, we briefly sketch the evaluation of ground-state expectation values for quantum systems resulting from a given Langevin equation.[10] For this purpose, we introduce the norm of the ground-state wave function,

$$N=\int dx_1\cdots dx_N\,\varphi_0^2(x_1,\ldots,x_N)$$
$$=\int dx_1\cdots dx_N \exp\left[-\frac{2W}{\sigma}\right] . \tag{26}$$

Knowledge of the φ_0 also allows the expression of ground-state expectation values in terms of multiple integrals,

$$\langle 0\mid A(x_1,\ldots,x_N)\mid 0\rangle=\frac{\int\prod_{i=1}^{N} dx_i A(x_1,\ldots,x_N)\varphi_0^2}{\int\prod_{i=1}^{N} dx_i\varphi_0^2} . \tag{27}$$

Next, we note the equivalence of N with the classical partition function of a system with potential energy W at temperature $2/\sigma=1/k_BT$. Similarly, the ground-state expectation value (27) is identical to the ensemble average of a classical system with potential energy W. Thus, the problem of evaluating ground-state expectation values for the quantum system resulting from the Langevin equation (1), is equivalent to the calculation of the partition function and ensemble averages of the classical model with potential energy W.[7] This equivalence is particularly appealing in one-dimensional many-particle systems, where the resulting multiple integrals can be treated with the transfer-integral technique, originally developed to calculate the partition function and related properties for classical systems.[11]

We are now prepared to specify the models and to list some of their ground-state expectation values.

A. Generalized quantum Toda lattice

The potential energy of the one-dimensional Toda lattice might be written as[12]

$$W=\frac{1}{g^2}\sum_l\{\exp[-g(x_{l+1}-x_l)]+g(x_{l+1}-x_l)-1\} . \tag{28}$$

In the weak coupling limit ($g\ll 1$), W reduces to the potential-energy expression of the harmonic chain. Using Eqs. (7), (8), and (28), a generalized quantum Toda chain with known ground-state wave function and energy [Eq. (10)] is now easily constructed. Its Hamiltonian is

$$\mathcal{H}=\sum_l\frac{\dot{x}_l^2}{2\sigma}+\tfrac{1}{2}\sum_l\left[\frac{1}{\sigma g^2}\{\exp[-g(x_{l+1}-x_l)]-\exp[-g(x_l-x_{l-1})]\}^2-\{\exp[-g(x_{l+1}-x_l)]+\exp[-g(x_l-x_{l-1})]\}\right] . \tag{29}$$

The potential energy not only involves nearest-neighbor but also next-nearest-neighbor interactions. Considering a lattice with one open end, the norm as obtained from Eqs. (26) and (28) is

$$N(p)=\int dx_0 dx_N \exp\left[-\frac{2}{\sigma}p(x_N-x_0)\right]$$
$$\times\int dx_1\cdots dx_{N-1}\exp\left[-\frac{2}{\sigma}\sum_{l=1}^{N-1}K_{l+1,l}\right] , \tag{30}$$

where

$$K_{l+1,l}=g^{-2}\{\exp[-g(x_{l+1}-x_l)]+g(x_{l+1}-x_l)-1\} \tag{31}$$

and p denotes the pressure. Evaluation of the multiple integral is completely equivalent to calculation of the partition function of the classical Toda lattice with potential energy W [Eq. (28)].[13] Introducing the variables

$$r_l=x_{l+1}-x_l , \tag{32}$$

and observing that

$$\partial(x_0,\ldots,x_N)/\partial(r_0,\ldots,r_N)=1 , \tag{33}$$

the multiple integral reduces to

$$N(p)=[n(\bar{p})]^N , \tag{34}$$

where

$$n(\bar{p})=g^{-1}e^{\beta}\beta^{-\beta(1+\bar{p})}\Gamma[(1+\bar{p})\beta]$$
$$=g^{-1}e^{\beta}\int_0^{\infty}dy\exp\{-\beta[(e^{-y}+y(\bar{p}+1))]\} . \tag{35}$$

Here, we have introduced the scaled variables

$$y=gr,\quad \bar{p}=pg,\quad \beta=2/\sigma g^2 . \tag{36}$$

Ground-state properties are now readily obtained. Examples are the zero-pressure linear expansion

$$g\langle r\rangle=\langle y\rangle=\beta^{-1}\frac{\partial\ln[n(\bar{p})]}{\partial\bar{p}} \tag{37}$$

and the zero-pressure mean-square expansion

$$g^2(\langle r^2\rangle-\langle r\rangle^2)=\beta^{-2}\frac{\partial^2\ln[n(\bar{p})]}{\partial\bar{p}^2} . \tag{38}$$

In the weak-coupling limit ($g\ll 1$), these expressions reduce to[14]

$$\langle r\rangle\mid_{p=0}=\tfrac{1}{4}\sigma g+\tfrac{1}{8}\sigma^2g^3-\tfrac{1}{1920}\sigma^4g^7 \tag{39}$$

and

$$\langle r^2\rangle-\langle r\rangle^2\mid_{p=0}=\tfrac{1}{2}\sigma+\tfrac{1}{8}\sigma^2g^2+\tfrac{1}{48}\sigma^3g^4 . \tag{40}$$

Clearly, in the weak-coupling limit the harmonic approximation becomes valid. The dynamic form factor for the

displacement fluctuations reduces to that of the harmonic chain

$$S_{xx}(q,w)=\sum_n |\langle 0|x(q)|n\rangle|^2\delta(\omega-\lambda_n)$$
$$\simeq\frac{\sigma}{2\omega(q)}\delta(\omega-\omega(q)) , \quad (41)$$

where

$$x(q)=\frac{1}{\sqrt{N}}\sum_l x_l e^{iqal} , \quad (42)$$
$$\omega(q)=2[1-\cos(qa)] , \quad (43)$$
$$a=\pi+\langle r\rangle|_{p=0} . \quad (44)$$

The lattice constant is a, the quasiharmonic phonon frequency $\omega(q)$, and $-\pi/a\le q\le\pi/a$ denotes the wave number. The Langevin simulation of this quantum Toda model will then provide estimates for the imaginary-time analog

$$S_{xx}(q,t)=\sum_n |\langle 0|x(q)|n\rangle|^2 e^{-\lambda_n t} , \quad (45)$$

yielding, from the long-time behavior, estimates for the phonon frequency. It is important to emphasize that the simulation is not restricted to the weak coupling limit. In fact, a crucial question is how the phonon frequency varies with the strength of the coupling constant g.

B. Generalized sine-Gordon chain

As a second example, we construct a generalized sine-Gordon chain with a potential energy of

$$W=\frac{A}{g^2}\sum_l[1-\cos(gx_l)]+\frac{c}{2}\sum_l(x_{l+1}-x_l)^2 , \quad (46)$$

where g is the coupling constant. For $g\ll 1$, this expression reduces to the potential energy of the harmonic chain. Invoking then Eqs. (7), (8), and (46) for the Hamiltonian of the generalized quantum sine-Gordon chain, we find

$$\mathcal{H}=\sum_l\frac{\dot{x}_l^2}{2\sigma}+\frac{1}{2\sigma}\sum_l\left[\frac{A}{g}\sin(gx_l)+C(2x_l-x_{l+1}-x_{l-1})\right]^2$$
$$-\tfrac{1}{2}\sum_l[A\cos(gx_l)+2C] , \quad (47)$$

with known ground-state wave function and eigenvalue [Eq. (10)]. The calculation of the norm

$$N(A,C,\sigma,g)=\int\prod_l dx_l e^{-2W/\sigma} \quad (48)$$

is again equivalent to the evaluation of the classical partition function of the sine-Gordon chain, with $1/k_BT$ replaced by $2/\sigma$. As a consequence, the transfer-integral technique can be used to calculate properties of interest.[14] For

$$C/A\gg 1,\quad 1/\beta C\gg 1,\quad \beta=2/\sigma g^2 , \quad (49)$$

the resulting Fredholm integral equation can be transformed into an eigenvalue problem of Mathieu form. For

$$128AC/\sigma^2 g^4\gg 1 , \quad (50)$$

corresponding to the weak-coupling limit ($g\ll 1$), asymptotic expansions are well documented,[14,15] yielding, for example,

$$\langle\cos(gx_l)\rangle=1-\frac{2}{\beta E_k}-\frac{1}{2(\beta E_k)^3}+\cdots+O(\exp(-\beta E_k)) , \quad (51)$$

$$S_{cc}(q,0)=\frac{1}{\beta A}\left[\frac{1}{\beta E_k}+\frac{3}{2^2(\beta E_k)^3}+\cdots\right]+O(\exp(-\beta E_k)) , \quad (52)$$

$$\lim_{q\to 0}q^2 S_{xx}(q)=\frac{32A\beta}{g^2}\frac{1}{8}(\beta E_k)^{1/2}\exp(-\beta E_k) , \quad (53)$$

where

$$E_k=8(AC)^{1/2} ,$$
$$S_{cc}(q)=\langle|N^{-1/2}\sum_l e^{iql}[\cos(gx_l)]-\langle\cos(gx_l)\rangle|^2\rangle , \quad (54)$$
$$S_{xx}(q)=\langle|N^{-1/2}\sum_l e^{iql}x_l|^2\rangle .$$

E_k is the kink-soliton energy of the classical chain. Other ground-state properties might be obtained from the numerical and analytical transfer-integral results of the classical sine-Gordon chain.[15]

Comparison of the weak-coupling results for the generalized quantum Toda [Eqs. (39) and (40)] and quantum sine-Gordon [Eqs. (51) and (53)] chains reveals important differences. In the Toda case, perturbation theory will work, because in the weak-coupling limit the ground-state properties are given by a power-law expansion in the coupling constant, which can be collected in terms of derivatives of the Γ function [Eqs. (37) and (38)]. In the sine-Gordon case, one has to distinguish between properties dominated by power laws and those where the exponential contribution, originating in the classical case from the kink solitons, enters to leading order. In fact, for properties dominated by the exponential term, the weak-coupling limit ($g\to 0$) corresponds to an essential singularity, so that perturbation theory is not applicable. For power-law dominated properties, however, usual perturbation theory is again valid.

Here, we consider the dynamic form factor

$$S_{cc}(q,\omega)=\sum_n\left|\left\langle 0\left|\frac{1}{\sqrt{N}}\sum_l e^{iql}[\cos(gx_l)-\langle\cos(gx_l)\rangle]\right|n\right\rangle\right|^2\delta(\omega-\lambda_n) , \quad (55)$$

where perturbation theory should be applicable. In analogy to the quantum sine-Gordon system, the weak-coupling limit is expected to be obtained by a two-phonon bound state, followed by the two-phonon continuum.[16] A weak-coupling treatment of the generalized quantum sine-Gordon system yields, for the bound-state frequency,[10]

$$\omega(q=0)=2\Omega(0)\left[1-\left[\frac{g^2\sigma}{4(2CA)^{1/2}}\frac{(1+\sigma g^2/8A)^2}{1+\sigma g^2/2A}\right]^2\right]^{1/2}, \tag{56}$$

where the phonon frequency is given by

$$\Omega^2(q)=[A+2C(1-\cos(q))]^2+\tfrac{1}{2}\sigma g^2 A\ . \tag{57}$$

The Langevin simulation will then provide estimates for the imaginary-time analog:

$$S_{cc}(q,t)=\sum_n\left|\left\langle 0\left|\frac{1}{\sqrt{N}}\sum_l e^{iql}[\cos(gx_l)-\langle\cos(gx_l)\rangle]\right|n\right\rangle\right|^2 e^{-\lambda_n t}, \tag{58}$$

yielding, from the long-term behavior, estimates for the bound-state frequency. This will allow checking of the range of validity of the weak-coupling prediction [Eq. (56)].

C. Free impenetrable bosons on a ring

Free impenetrable bosons on a ring and spinless fermions share many common properties. Girardeau has shown that the excitation spectrum of the two systems are identical as all configurational probability distributions.[7] The ground-state wave function is given by

$$\varphi_0=(N!)^{1/2}L^{-N/2}2^{N(N-1)/2}\prod_{\substack{j,l\\ j>l}}\left|\sin\frac{\pi}{L}(x_j-x_l)\right|. \tag{59}$$

The structure of this wave function reveals that, if we vary the position of one particle, keeping all the others fixed, then the wave function will be positive and smoothly varying everywhere except at the position of the other particles, where it vanishes and has a cusp as a result of the singular repulsive interaction, or in the case of fermions, owing to the Pauli principle. As a consequence, the classical potential

$$W=-\sigma\ln\varphi_0 \tag{60}$$

entering the Langevin equation, becomes infinite between equilibrium positions of the particles. This suggests that the classical Langevin analog forms a lattice, and the particles will fluctuate around their equilibrium positions.

Given the wave function (59), the Langevin equations (1), allowing simulation of this system, read

$$\dot{x}_l=\frac{\sigma\pi}{L}\sum_{j(\neq l)}\cot\left[\frac{\pi}{L}(x_l-x_j)\right]+\eta_l(t),\quad l=1,\ldots,N\ . \tag{61}$$

Of interest are then the trajectories $x_l(t)$ and the long-time dependence of the correlation function

$$S_{\rho\rho}(q,t)=\sum_n|\langle 0|\rho(q)|n\rangle|^2 e^{-\lambda_n t}, \tag{62}$$

where

$$\rho(q)=\frac{1}{\sqrt{N}}\sum_l e^{iqx_l}\ . \tag{63}$$

The excitations correspond to particle-hole pairs with energy[16]

$$\omega(k_n,q)=\frac{\sigma}{2}(q^2+2k_nq)\ . \tag{64}$$

For a finite system, the wave number k_n can adopt the values

$$k_n=n\frac{2\pi}{L},\quad n=\pm1,\ldots,\pm\tfrac{1}{2}N\ , \tag{65}$$

where $n=\pm N/2$ corresponds to the Fourier wave number

$$k_F=\frac{N}{L}\pi \tag{66}$$

at the Fermi level. The allowed excitations correspond to particle-hole pairs with energy $\omega(k_n,q)$, bounded by

$$|k_F^2-(k_F-q)^2|\leq\omega(k_n,q)\leq|(k_F+q)^2-k_F^2|\ . \tag{67}$$

For $q<2k_F$ and taking requirement (67), Eq. (62) reduces to

$$S_{\rho\rho}(q,t)=\frac{1}{N}\sum_{\substack{n=[N/2-gL/2\pi]+1\\ (n\neq0)}}^{N/2}\exp\left[-\frac{\sigma}{2}(q^2+q\frac{4\pi}{L}n)t\right]. \tag{68}$$

Here, $[x]$ denotes the largest integer smaller than or equal to x. For the infinite system, Eq. (68) yields

$$S_{\rho\rho}(q,t)=\frac{\sinh(\frac{1}{2}\sigma q^2 t)}{\pi\rho\sigma q t}\exp(-\sigma q k_F t)\ , \tag{69}$$

where the sum over n has been replaced by an integral, and the density of fermions $\rho=N/L$ is kept constant. Similarly, we find for $q>2k_F$,

$$S_{\rho\rho}(q,t)=\frac{1}{N}\sum_{\substack{n=-N/2\\ (n\neq0)}}^{N/2}\exp\left[-\frac{\sigma}{2}\left[q^2+q\frac{4\pi}{L}n\right]t\right], \tag{70}$$

reducing for the infinite system to

$$S_{\rho\rho}(q,t)=\frac{\exp(-\frac{1}{2}\sigma q^2 t)}{\pi\rho\sigma q t}\sinh(\sigma q k_F t)\ . \tag{71}$$

Replacing t by it yields for the dynamic density form factor of the quantum problem,

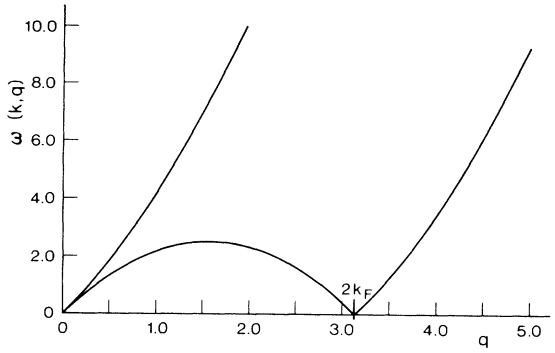

FIG. 1. Boundaries of the particle-hole continuum for a system consisting of $N=20$ particles in a box of length $L=40$, $\sigma=2$, and $k_F=N/L\pi=\pi/2$. The shaded region shows the allowed excitation frequencies.

$$S_{\rho\rho}(q,\omega)=\frac{1}{N}\sum\delta(\omega-\omega(k_n,q)) , \tag{72}$$

where

$$|k_F^2-(k_F-q)^2| \leq \omega(k_n,q) \leq |(k_F+q)^2-k_F^2| . \tag{73}$$

The particle-hole continuum and its boundaries are shown in Fig. 1. At the boundaries, $S_{\rho\rho}(q,\omega)$ exhibits a discontinuity, giving rise to the nontrivial time dependence of the imaginary-time density correlation functions [Eqs. (69) and (71)] for the infinite system.

III. NUMERICAL RESULTS

In this section, we present numerical results for the three models described above, namely, (i) the generalized Toda chain, (ii) the generalized sine-Gordon chain, and (iii) the system of free impenetrable bosons or spinless fermions on a ring. In all three cases, correlation functions have been obtained by numerical simulation to extract information about the eigenvalue spectrum. For a description of the numerical method used, the reader is referred to the Appendix.

In the Toda case, the Langevin equation (1) was solved numerically with periodic boundary conditions, and using the initial condition $x_l=0$, $l=1,2,\ldots,N$. The time increment in the Euler scheme was set to $\Delta t=0.01$, and the correlation function was calculated using 4096 time points with a sampling interval equal to $\Delta T=0.2$. The lowest eigenvalue, as probed by the displacement correlation function, was estimated from the long-time behavior and by averaging over 30 independent runs. The resulting dispersion curves $\lambda_1(q_{\rm red})=\omega(q_{\rm red})$ are shown in Fig. 2 for a chain of 100 particles subjected to periodic boundary conditions. For comparison, we included the weak-coupling prediction [Eq. (43)]:

$$\omega(q_{\rm red})=2[1-\cos(\pi q_{\rm red})] , \tag{74}$$

where

$$q_{\rm red}=\frac{a}{\pi}q=q+\frac{q}{\pi}\langle r\rangle\,|_{p=0} , \tag{75}$$

$\langle r\rangle_{p=0}$ denoting the zero pressure expansion [Eq. (37)].

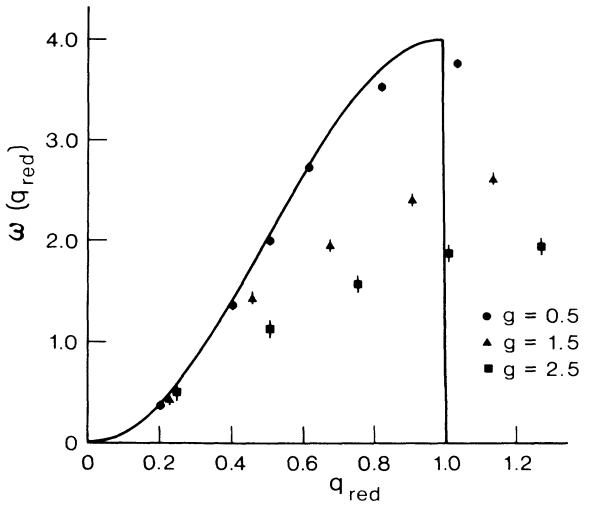

FIG. 2. Numerical estimates for the phonon frequencies of the generalized Toda chain [Eq. (29)] from the Langevin simulation of $S_{xx}(q,t)$. For comparison, we include the weak-coupling prediction [Eq. (75)] (solid curve). Simulations for three different values of the coupling constant g are shown: ●, $g=0.5$; ▲, $g=1.5$; and ■, $g=2.5$.

For $g=0.5$ and $q_{red}<0.7$, the weak-coupling prediction [Eq. (74)] agrees well with the numerical estimates. As the coupling constant is increased, the $q_{\rm red}$ range, where agreement with the weak-coupling result is obtained, is seen to shrink and move toward smaller $q_{\rm red}$ values. In fact, nonlinear effects can no longer be neglected.

Finally, we note that by rescaling the Langevin equation (1) in terms of $\varphi_l(t)=gx_l(t)$, the coupling constant g can be absorbed in the effective variance $\sigma_{\rm eff}=g^2\sigma$ of the random force.

For the sine-Gordon chain, we also used the Euler scheme with time steps $\Delta t=0.01$. Estimates for the bound-state frequency $\lambda_1(q=0)=\omega(q=0)$ [Eq. (56)] were obtained from the correlation function $S_{cc}(q,t)$ [Eq. (58)] using 4096 time points with a sampling interval $\Delta T=0.1$. Tests were also performed with 16 384 time points, confirming the reliability of the shorter runs. The numerical estimates for the bound-state frequency $\omega(q=0)$, averaged over 20 independent runs, and its coupling-constant dependence are shown in Fig. 3 for a system of 200 particles subjected to periodic boundary conditions. The values of the parameters were chosen as follows: $\sigma=8.924$, $A=1$, and $C=29.22$. Comparison reveals that the weak-coupling approximation (56) provides reliable estimates for $g\lesssim 0.2$; it fails for stronger couplings.

In analogy to the Toda chain, the Langevin equation for the sine-Gordon chain can be scaled by means of $\varphi_l(t')=gx_l(t)$ and $t'=At$. The effective variance of the quantum fluctuation then becomes $\sigma_{\rm eff}=\sigma g^2/A$. Thus, a change of the coupling constant g is equivalent to a change of $\sigma_{\rm eff}$. It is seen, however, that this scaling only holds for fixed A because A still appears as a factor in the harmonic term in the scaled Langevin equation.

In the numerical simulations of the free fermions, we have considered a system of $N=20$ particles in a box of

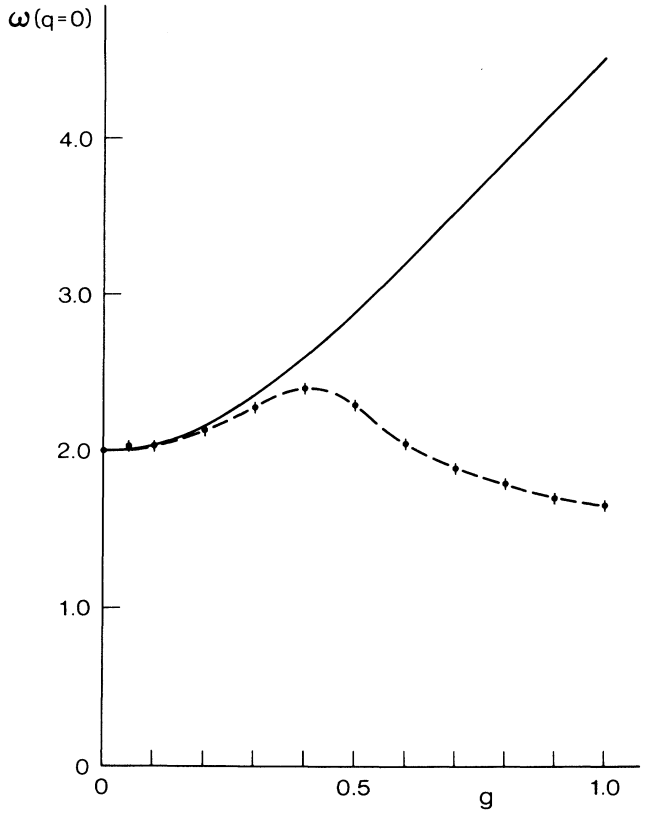

FIG. 3. Numerical estimates of the generalized sine-Gordon equation [Eq. (47)] for the two-phonon bound-state frequency $\omega(q=0)$ [Eq. (56)] obtained from Langevin simulation of $S_{cc}(q,t)$ [Eq. (58)] for $A=1$, $C=29.22$, and $\sigma=8.924$. The solid curve represents the weak-coupling approximation [Eq. (56)], the dashed curve the numerical estimate.

length $L=40$ ($-L/2\leq x\leq L/2$). The Langevin equation (61) was solved using the Euler scheme with $\sigma=2$ and using time steps $\Delta t=0.005$. In Fig. 4, we show the trajectories of the classical particles obtained from the Langevin equation, initially uniformly distributed, after the system has relaxed to equilibrium. It is clearly seen that the system forms a lattice with spacing $a=1/\rho$. The time evolution is governed by oscillations around the equilibrium positions. This reflects the infinitely high barriers between particles [Eq. (61)] arising from the zeros of the ground-state wave function, expressing the impenetrability of the bosons, or the Pauli principle for spinless fermions. In the numerical scheme, the repulsive force between two particles is assumed constant over one time step. Therefore, if two particles come sufficiently close to each other, crossing may occur owing to the random force. To avoid such artificial crossing, we impose a small separation $\Delta x=0.25\sqrt{\sigma\Delta t}$ on two particles, a distance less than Δx apart. If the particles exceed the box length L the entire system will be compressed to a size equal to L. Finally, the mean position of the particles is subtracted in each time step, to avoid possible artificial drift of the center of mass.

With the exact expression for $S_{\rho\rho}(q,t)$ [Eqs. (68) and

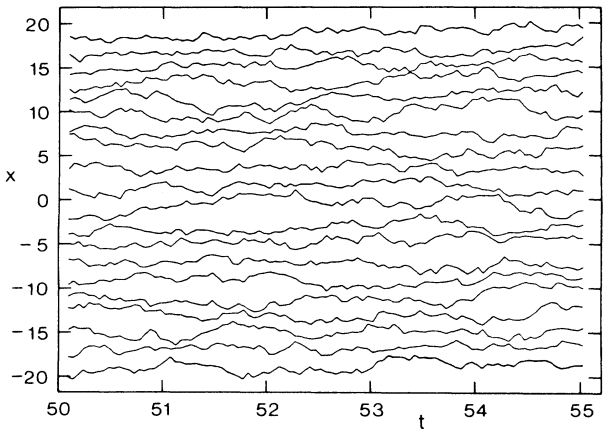

FIG. 4. Trajectories of $N=20$ particles evolving according to the Langevin equation (61) and corresponding to the classical analog of impenetrable bosons or free fermions on a ring with $L=40$ and $\sigma=2$. The particles form a lattice with lattice constant $\alpha=L/N=2$.

(70)], we are in a position to test the numerical simulations. Figure 5 shows a comparison between the exact expression for $S_{\rho\rho}(q,t)$ and the corresponding simulation results for $q=1.2\pi$. We plotted the analytic result for $\ln[S_{\rho\rho}(q,t)/S_{\rho\rho}(q,0)]$ (solid line) and its dominating long-time term (dashed line) [Eq. (70)] versus time t. The dots denote the numerical estimates where we have averaged over 88 independent runs. The correlation functions were calculated using 65 536 points with a sampling interval $\Delta T=0.05$. Up to the time $t\approx 1.4$, the numerical and analytic results agree well. From Fig. 5, it is seen however, that much longer times are needed to extract the first eigenvalue λ_1 from the long-time behavior. It should be kept in mind however, that for the infinite system, the long-time behavior is no longer governed by an exponential decay [Eqs. (69) and (71)].

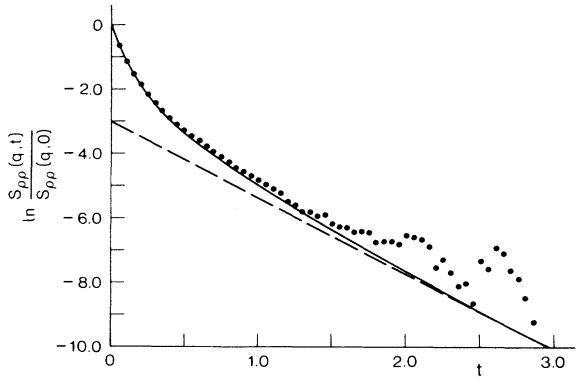

FIG. 5. Plot of $\ln[S_{\rho\rho}(q,t)/S_{\rho\rho}(q,0)]$ for a system for $N=20$ impenetrable bosons with $\rho=N/L=\frac{1}{2}$ and $\sigma=2$. The dots are numerical results, the solid line denotes the analytic prediction [Eq. (70)] and the dashed line indicates the dominating long-time behavior.

APPENDIX: NUMERICAL METHOD

We have solved the Langevin equation (1) by means of the explicit finite difference scheme

$$x_l^{n+1}=x_l^n+F_l(\mathbf{x}^n)\Delta t+\eta_l^n\Delta t,\quad l=1,2,\ldots,N\ , \tag{A1}$$

where x_l^n is an approximation to the original function $x_l(t_n)$ at the time $t_n=n\Delta t$, $n=0,1,2,\ldots$, and with the time increment Δt.[17,18] N is the number of particles, and $F_l(\mathbf{x}^n)=-\partial W(\mathbf{x}^n)/\partial x_l^n$ is the force acting on particle l in a potential $W(\mathbf{x})$. Here, $\mathbf{x}$ denotes the vector $(x_1^n,\ldots,x_N^n)$. η_l^n is the discretized random force treated in further detail below.

The above scheme is known as the Euler method. However, a more precise method for deterministic equations is the so-called Heun scheme[19] which is a predictor-corrector method. First, a solution $x_l^{n+1,0}$ is predicted by the Euler scheme (A1). Thereafter, a finite sequence of iterates $x_l^{n+1,s}$, $s=1,2,\ldots,S_{\max}$ are constructed by

$$X_l^{n+1,s}=x_l^n+\tfrac{1}{2}[F_l(\mathbf{x}^n)+F_l(\mathbf{x}^{n+1,s-1})]\Delta t+\eta_l^n\Delta t\ . \tag{A2}$$

Here, $x_l^n=x_l^{n,S_{\max}}$ is the previously computed point, and $S_{\max}$ can be set to 2 or 3 for practical purposes. In the three examples we have studied, namely, the Toda lattice, the sine-Gordon lattice, and the system of free fermions in one dimension, the Euler method has proven to give reliable results, and using the Heun method was not necessary. One should recall that iterations (A2) cost computer time and unless high accuracy is needed or considerably longer time steps can be used in the Heun scheme, the Euler method will be satisfactory.

The random forces $\eta_l(t)$ in the Langevin equation (1) satisfy $\langle\eta_l(t)\rangle=0$ and $\langle\eta_l(t)\eta_{l'}(t')\rangle=\sigma\delta_{ll'}\delta(t-t')$. In the numerical scheme, the δ function is approximated by a square function of width Δt and height $1/\Delta t$ placed symmetrically around $t'=n'\Delta t$. Hence, in the discrete case, $\eta_l^n=\eta_l(t_n)$ are Gaussian distributed random numbers obeying $\langle\eta_l^n\rangle=0$ and $\langle\eta_l^n\eta_{l'}^{n'}\rangle=\sigma/\Delta t\,\delta_{ll'}\delta_{nn'}$. The η_l^n can be constructed using the central limit theorem. Let U_{lk}^n be equally distributed random numbers in the interval [0,1] with expectation value $\langle U_{lk}^n\rangle=\frac{1}{2}$, and correlation

$$\langle(U_{lk}^n-\tfrac{1}{2})(U_{l'k'}^{n'}-\tfrac{1}{2})\rangle=\tfrac{1}{12}\delta_{nn'}\delta_{ll'}\delta_{kk'}\ .$$

In accordance with the central limit theorem, the variables g_l^n defined by[20]

$$g_l^n=\sum_{k=1}^{M}U_{lk}^n-\tfrac{1}{2}M \tag{A3}$$

are Gaussian distributed for large M. For practical purposes, M is chosen to be 12 which leads to very small absolute deviations in the tails of the distribution. From Eq. (A3), we easily see that $\langle g_l^n\rangle=0$, $\langle g_l^n g_{l'}^{n'}\rangle=\delta_{nn'}\delta_{ll'}$, and accordingly the Gaussian distributed random numbers η_l^n are determined by

$$\eta_l^n=\sqrt{\sigma/\Delta t}\,g_l^n\ . \tag{A4}$$

The equally distributed random numbers U_{lk}^n are obtained by using a standard pseudorandom number generator.[21]

After having solved the Langevin equation numerically for some appropriate initial conditions, time correlation functions of the form $\langle x(q,t)x(-q,0)\rangle$ have to be calculated. Assuming the system to be ergodic, the canonical averages may be replaced by time averages, i.e.,

$$S_{xx}(q,t)=\langle x(q,t)x(-q,0)\rangle=\langle x(q,t+t')x(-q,t')\rangle$$

$$=\lim_{\tau\to\infty}\frac{1}{\tau-t}\int_0^{\tau-t}x(q,t+t')x(-q,t')dt'\ . \tag{A5}$$

Hereby, $S_{xx}(q,t)$ is expressed as a convolution integral[17] and can be calculated by taking the Fourier transform $x(q,\omega)$ of $x(q,t)$ followed by an inverse Fourier transformation of $|x(q,\omega)|^2$ whereby $S_{xx}(q,t)$ is obtained. As the above Fourier transformations can be performed using the fast Fourier-transform method, time correlation functions are computed very efficiently.

---

*Present address: Institut für Theoretische Physik, Schönberggasse 9, 8001 Zurich, Switzerland.

[1]N. G. van Kampen, J. Stat. Phys. **17**, 71 (1977); N. S. Goel, S. C. Maitra, and E. W. Montroll, Rev. Mod. Phys. **43**, 231 (1981).
[2]G. Parisi and Y. S. Wu, Sci. Sin. **24**, 483 (1981).
[3]J. R. Klauder, Phys. Rev. A **29**, 2036 (1984).
[4]T. Schneider, M. Zannetti, R. Badii, and H. R. Jauslin, Phys. Rev. Lett. **53**, 2191 (1984).
[5]T. Schneider, M. Zannetti, and R. Badii, Phys. Rev. B **31**, 2941 (1985).
[6]D. M. Ceperley and M. H. Kalos, in *Monte Carlo Methods in Statistical Physics*, edited by K. Binder (Springer, Heidelberg, 1979).
[7]M. Girardeau, J. Math. Phys. **6**, 516 (1960).
[8]A. Aharony, E. Domany, R. H. Hornreich, T. Schneider, and M. Zannetti, Phys. Rev. B **32**, 3358 (1985).
[9]T. Schneider and M. Schwartz, Phys. Rev. B **31**, 7484 (1985).
[10]T. Schneider and R. Badii, J. Phys. A **18**, L187 (1985).
[11]D. J. Scalapino, M. Sears, and R. A. Ferrell, Phys. Rev. B **6**, 3409 (1972).
[12]M. Toda, J. Phys. Soc. Jpn. **24**, 431 (1967).
[13]H. Takahashi, Proc. Math. Soc. Jpn. **24**, 60 (1942).
[14]T. Schneider and E. Stoll, in *Physics in One Dimension*, edited by J. Bernasconi and T. Schneider (Springer, Heidelberg, 1981), p. 75.
[15]T. Schneider and E. Stoll, Phys. Rev. B **22**, 5317 (1980).
[16]D. Pines and P. Nozieres, *The Theory of Quantum Liquids* (Benjamin, New York, 1966).
[17]R. H. Morf and E. P. Stoll, in *Numerical Analysis*, edited by J. Descloux and J. Marti (Birkhauser, Basel, 1977), Vol. 37, p. 139.
[18]T. Schneider and E. P. Stoll, Phys. Rev. B **17**, 1302 (1978).
[19]W. Rümelin, Forschungsschwerpunkt Dynamische Systeme, Universität Bremen, Report No. 12, 1980 (unpublished).
[20]N. Garcia and E. P. Stoll, Phys. Rev. Lett. **52**, 1798 (1984).
[21]S. Kirkpatrick and E. P. Stoll, J. Comput. Phys. **40**, 517 (1981).